Reliable solution processed planar perovskite hybrid solar cells with large-area uniformity by chloroform soaking and spin rinsing induced surface precipitation

Yann-Cherng Chern, Hung-Ruei Wu, Yen-Chu Chen, Hsiao-Wen Zan, Hsin-Fei Meng, and Sheng-Fu Horng

---

Articles you may be interested in

Evaluation of the reliability of commercial concentrator triple-junction solar cells by means of accelerated life tests (ALT)
AIP Conf. Proc. **1556**, 222 (2013); 10.1063/1.4822236

CPV infant mortality and indoor characterization for high efficiency, reliable solar cells
AIP Conf. Proc. **1556**, 6 (2013); 10.1063/1.4822186

Observation of metal precipitates at prebreakdown sites in multicrystalline silicon solar cells
Appl. Phys. Lett. **95**, 232113 (2009); 10.1063/1.3272682

Impact of metal silicide precipitate dissolution during rapid thermal processing of multicrystalline silicon solar cells
Appl. Phys. Lett. **87**, 121918 (2005); 10.1063/1.2048819

Nanometer-scale metal precipitates in multicrystalline silicon solar cells
J. Appl. Phys. **89**, 4282 (2001); 10.1063/1.1330552

Reliable solution processed planar perovskite hybrid solar cells with large-area uniformity by chloroform soaking and spin rinsing induced surface precipitation

Yann-Cherng Chern,[1] Hung-Ruei Wu,[1] Yen-Chu Chen,[1] Hsiao-Wen Zan,[2] Hsin-Fei Meng,[3] and Sheng-Fu Horng[1,a]

[1]*Department of Electrical Engineering and Institute of Electronics Engineering, National Tsing Hua University, Hsinchu, Taiwan 30013, ROC*
[2]*Department of Photonics and Institute of Electro-Optical Engineering, National Chiao Tung University, Hsinchu, Taiwan 30010, ROC*
[3]*Institute of Physics, National Chiao Tung University, Hsinchu, Taiwan 30010, ROC*

A solvent soaking and rinsing method, in which the solvent was allowed to soak all over the surface followed by a spinning for solvent draining, was found to produce perovskite layers with high uniformity on a centimeter scale and with much improved reliability. Besides the enhanced crystallinity and surface morphology due to the rinsing induced surface precipitation that constrains the grain growth underneath in the precursor films, large-area uniformity with film thickness determined exclusively by the rotational speed of rinsing spinning for solvent draining was observed. With chloroform as rinsing solvent, highly uniform and mirror-like perovskite layers of area as large as 8 cm × 8 cm were produced and highly uniform planar perovskite solar cells with power conversion efficiency of 10.6 ± 0.2% as well as much prolonged lifetime were obtained. The high uniformity and reliability observed with this solvent soaking and rinsing method were ascribed to the low viscosity of chloroform as well as its feasibility of mixing with the solvent used in the precursor solution. Moreover, since the surface precipitation forms before the solvent draining, this solvent soaking and rinsing method may be adapted to spinless process and be compatible with large-area and continuous production. With the large-area uniformity and reliability for the resultant perovskite layers, this chloroform soaking and rinsing approach may thus be promising for the mass production and commercialization of large-area perovskite solar cells. © 2015 Author(s). All article content, except where otherwise noted, is licensed under a Creative Commons Attribution 3.0 Unported License. [http://dx.doi.org/10.1063/1.4928516]

I. INTRODUCTION

Organometal halide perovskites solar cells (PSCs) are very promising for cost effective solar energy conversion and have attracted tremendous attention recently.[1] Remarkable progress on PSCs has been made and the highest certified power conversion efficiency (PCE) exceeds 20% to date.[2] PSCs can be structured in either mesosuperstructure-type[3,4] or planar-type.[5–7] Planar-type devices are particularly interesting because their simple layer design can be feasibly prepared with low-temperature processing.[5,6] Various methods have been developed for the preparation of the perovskite layers, including evaporation,[7,8] vapor-assisted solution process[9] and solution process in either one step.[5,10–15] or two steps[3,16,17] Among these different techniques, one-step solution processing is potentially the lowest-cost one and may be adaptable to large-area production. Combined with low-temperature solution processing, planar-type PSCs can be fabricated on low-cost, flexible

---

[a]sfhorng@ee.nthu.edu.tw

substrates to exploit the cost effectiveness of high throughput continuous fabrication technologies such as roll-to-roll processing.

It is well known that thick perovskite layers with large grain sizes, complete surface overage and smooth surface morphology are required to produce high-efficiency PSCs.[11,16–18] Improved planarity, which leads to higher uniformity in the active layer thickness, is also crucial for large-area PSCs because, like all other thin-film solar cells, large-area PSCs should be configured in cascaded structure of sub cells, which are limited in performance by the weakest link that deteriorates with increased non uniformity. Therefore, the simultaneous control over the crystallinity and the morphology of thick perovskite active layers is of paramount importance for the development of large-area PSCs. However, compared to vapor- or vacuum deposition methods, solution processing usually produces perovskite films with relatively small grain sizes, rough surface morphology and incomplete surface coverage.[3,7,8] This is especially the case for thick perovskite films prepared with a one-step solution deposition.[4,7,19] Solvent annealing was found to increase the grain sizes greatly, yet the difficulty with surface roughness remains.[16]

In 2014, Jeon *et al* employed a mixture of dimethyl sulfoxide (DMSO): γ-butyrolactone (GBL) as solvent for the precursors to retard their rapid reaction, allowing for a consecutive toluene dripping on the surface of the spinning as-coated films to obtain extremely uniform and dense perovskite layers. With this solvent engineering technique, or solvent washing process as was also referred, a PCE of 16.2% was obtained on a mesosuperstructure-type device.[4] Following this technique, Seok *et al* fabricated the planar p–i–n perovskite cell and achieved a PCE of 14.1% (11.5%) with LiF/Al (Al) as cathode.[11] Jung *et al* reported the use of washing solvent with larger dipole moment than toluene, and obtained with chlorobenzene (CB) an average PCE of 13.7% from planar devices.[6] Recently in 2015 Chen *et al* also reported their fabrication of planar PSCs, achieving a best PCE of 7.28% for their toluene washed devices. Furthermore, a PCE of 9.08% was achieved when a small molecule additive was used.[20] In essence, this solvent washing method is the formation of a surface precipitation layer by rinsing the surface of the as-coated perovskite layers with solvents that do not dissolve the precursors. The constraining surface precipitation layer then maintains the surface planarity and allows for large grain growth underneath in the perovskite layer, thus achieving simultaneous enhancement in both grain sizes and surface morphology for the resulted perovskite films. However, while this solvent washing method is remarkably effective in improving the surface morphology and crystallinity of the perovskite films, the droplet impact on the spinning surface strongly affects the thickness of the resultant perovskite layers and it is difficult to control the extent of solvent dripping, especially in the case of large-area devices. In addition, the solvent washing process requires spinning surfaces and involves complicated physical processes; it is therefore difficult to control and scale up.[21,22]

In this work, we report a modified surface rinsing method in which the rinsing solvent is allowed to soak the whole surface of the as-coated perovskite layer to form the precipitation before the treated films are subject to spinning to drain the solvents. Besides the enhanced crystallinity and surface morphology due to the rinsing induced surface precipitation that constrains the grain growth underneath in the precursor films, large-area uniformity with film thickness determined exclusively by the rotational speed of rinsing spinning for solvent draining was observed. With the use of chloroform (CF) in this solvent soaking and rinsing process, mirror-like perovskite layer of 8 cm × 8 cm was obtained and highly uniform planar PSC devices with PCE of $10.6 \pm 0.2\%$ and greatly enhanced reliability were achieved even with very simple layer structure of ITO/PEDOT:PSS/perovskite/$PC_{61}BM$/Al. Moreover, since the surface precipitation forms before the solvent draining, this solvent soaking and rinsing method may be adapted to spinless process and may thus be compatible with large-area and continuous production.

II. EXPERIMENTAL DETAILS

A. Materials and device fabrication

The process flow and device structure are shown in Fig. 1. Starting from 3 cm × 3 cm pre-cleaned Indium tin oxide (ITO) coated glass, Poly(3,4-ethylenedioxythiophene) Polystyrene
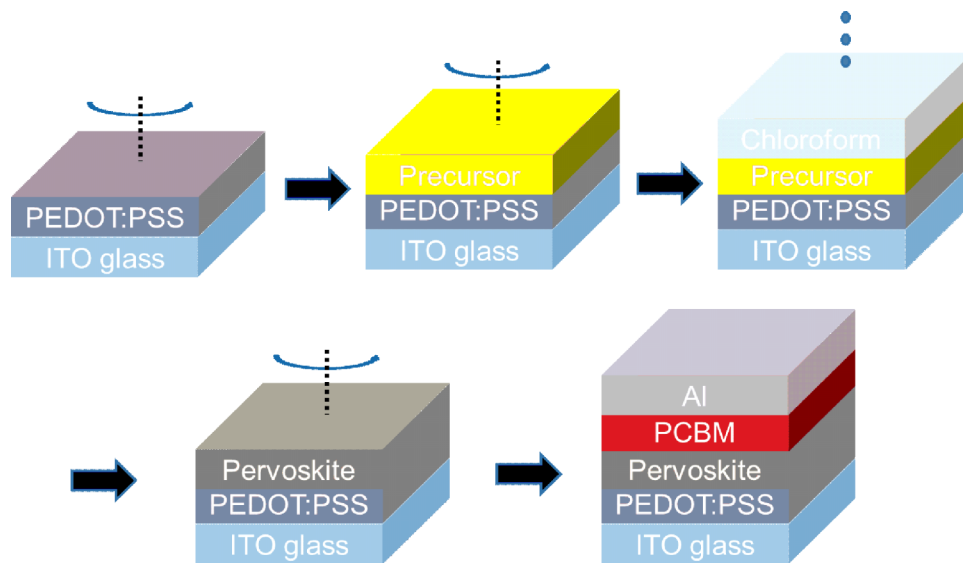
FIG. 1. Schematic illustration of the process flow and layer structure of the perovskite solar cells fabricated with CF soaking and rinsing spin.

sulfonate (PEDOT:PSS, AI4083, from Heraeus) was spin-coated at 3000 rpm and then annealed at 150°C for 15 min. To prepare the perovskite precursor solution, lead (II) chloride ($PbCl_2$, from Sigma-Aldrich) and Methylamine iodide (MAI, from Dyesol) were first dissolved in dimethylsulfoxide (DMSO) and N,N-Dimethylformamide (DMF) in 30wt%, respectively. After filtering, these two solutions were then mixed to form the precursor solution with a final concentration of 1.16M and 3.48M for $PbCl_2$ and MAI, respectively.

The precursor solution was then spin-coated onto the ITO/PEDOT:PSS layer at 2000 rpm for 5 sec and then 6000 rpm for 35 sec to form the perovskite precursor films. After the spinning stops, the rinsing solvent was applied to the surface and typical time duration around 15 sec was allowed for it to soak all over the whole surface of the as-coated precursor films. The rinsed films were then subject to spinning (referred as rinsing spinning in what follows) at different rotational speed and were then annealed at 90°C for different time duration to complete the crystal growth. As a reference, a control perovskite film without surface rinsing, which was annealed at 90°C for 100 min, was also prepared. To fabricate the PSCs, 2 wt% 6,6-phenyl-C61-butyric acid methyl ester ($PC_{61}BM$, from Nano-C) in CB was spin-coated onto the aforementioned prepared perovskite films at 1000 rpm for 60 sec, and were dried at room temperature for 2 hours. All the precursor spin coating and solvent rinsing processes were conducted in nitrogen-filled glove box. Subsequently, a top metal electrode of Aluminum (100 nm) was thermally deposited under a pressure of $3.5x10^{-6}$ torr. The fabricated devices were encapsulated using a UV-cured sealant and a cover glass under nitrogen ambient.

B. Characterizations

The SEM images were acquired using a Hitachi SU8010 Cold Field Emission Scanning Electron Microscope. The AFM images were obtained with a Force Genie atomic force microscope. The thickness of the films was measured using a Kosaka ET4000 3D profile and surface roughness measurement instrument. The X-ray diffraction was performed using a Bede D1 High Resolution X-Ray Diffractometer with Cu Kα1 radiation. The current density-voltage (*J–V*) characteristics of the devices were measured by Keithley 2400 source measurement unit using a San-Ei Electric XES 301S AM 1.5G solar simulator at 100 mWcm^{-2} calibrated by a Hamamatsu S1337-BR silicon photodiode. The external quantum efficiency (EQE) was conducted using a measurement system (model QE-R) built by Enli Technology.

III. RESULTS AND DISCUSSION

In our studies, toluene, CF, chlorobenzene (CB) and Acetone (ACE) were examined as the rinsing solvent, respectively. Among these solvents CB and ACE result in re-dissolution of the precursor films and do not produce perovskite films of sufficient smoothness for use in PSCs. This was attributed to the much longer time allowed for the washing solvent to effect morphological change, leading to very rough perovskite layers. On the other hand, the treatment with toluene and especially with CF does lead to mirror-like perovskite films. We will therefore focus on CF and later on toluene in what follows.

Both the as-coated and CF rinsed precursor films look transparent and colorless. They turn yellowish as the films are subject to annealing and then change to burgundy (or opaque dark brown) and finally become transparent dark brown, which is the characteristic color of the $CH_3NH_3PbI_3$ required for efficient PSCs. With our annealing at 90°C, it takes typically 60 min to complete the color change process. Our perovskite films were therefore subject to annealing at 90°C for 60, 80, 100 and 120 min, respectively. It is remarkable that it always takes more time for the CF rinsed films to change color at each stage. This is presumably due to the surface precipitation layer that retards the evaporation of the DMSO/DMF solvent mixture.

We can correlate the delayed color change for the CF rinsed perovskite films to their X-ray diffraction (XRD) characterization results as shown in Fig. 2. For the unrinsed perovskite layer, only characteristic peaks corresponding to $CH_3NH_3PbI_3$ (110), (220) and (310) at 14°, 28.4° and 31.8° can be identified, revealing that the transformation of the $PbCl_2$ and MAI precursors to $CH_3NH_3PbI_3$ is complete for the untreated film after annealing at 90°C for 100 min.[12] On the other hand, there is still minor signature of $CH_3NH_3PbCl_3$ (110) at 15.6[7] for the CF treated perovskite film annealed at 90°C for 100 min. Intriguingly enough, though all our spin-coating and CF rinsing were conducted in dry glove box, the XRD spectra and the decrease in $CH_3NH_3PbCl_3$ (110) peak with annealing (Fig. 1 and 2(d)) resemble closely the films prepared at controlled humidity of $30 \pm 5\%$ relative humidity [12.14]. Nevertheless, the observation of residual $CH_3NH_3PbCl_3$ signature can be understood by noting that both $CH_3NH_3PbI_3$ and $CH_3NH_3PbCl_3$ precipitate on the film surface quickly upon the contact with CF, and that much slower solid-state diffusion/reaction is required to consume $CH_3NH_3PbCl_3$ by annealing.
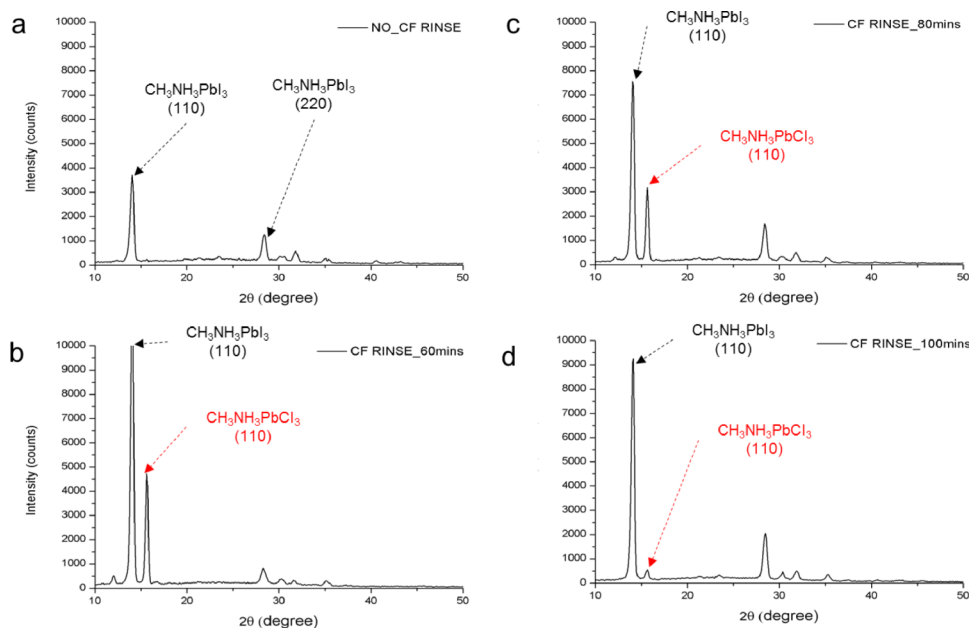

FIG. 2. XRD patterns obtained from perovskite layers (a) annealed at 90°C for 100 min without CF treatment, and with CF soaking and rinsing followed by annealing at 90°C for (b) 60 min, (c) 80 min and (d) 100 min. The CF spin rinsing speed is 6000 rpm.
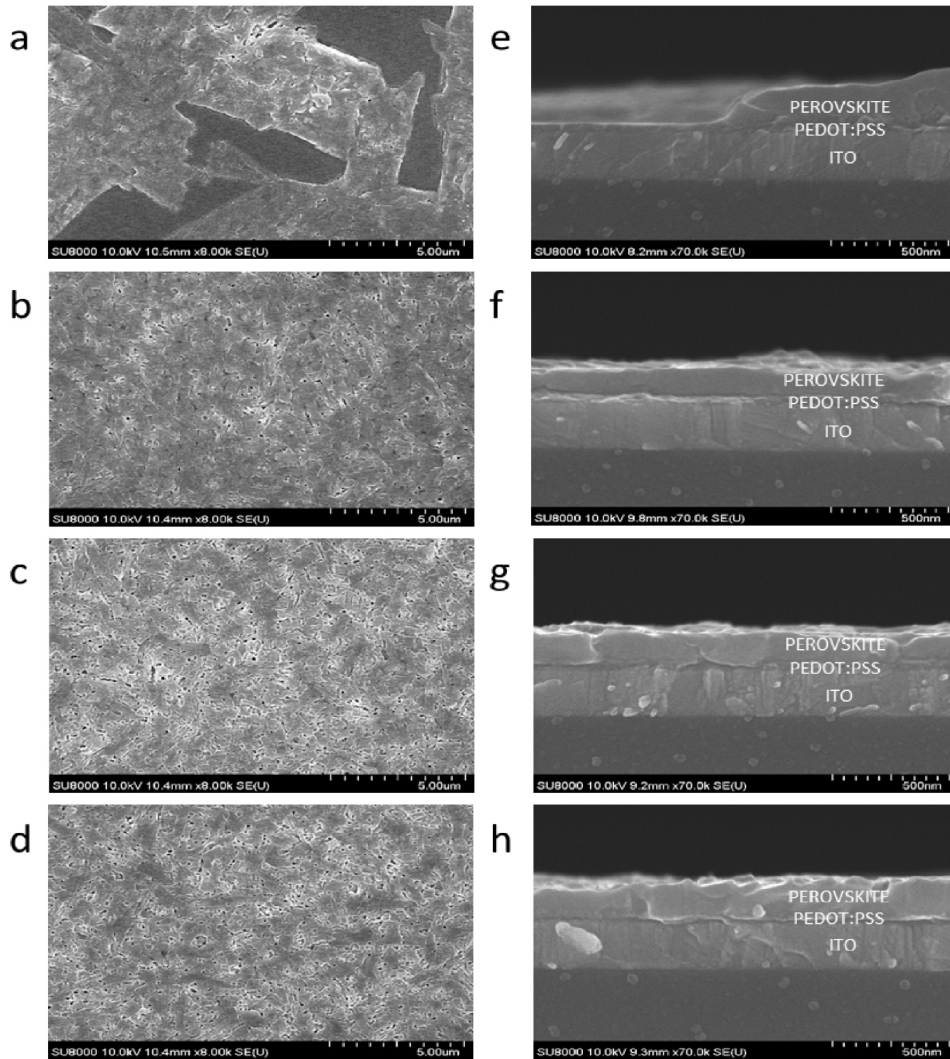
FIG. 3. (a-d) Top-view and (e-h) cross-sectional SEM images from perovskite layers (a,e) annealed at 90°C for 100 min without CF treatment, and with CF soaking and rinsing followed by annealing at 90°C for 80 min (b,f), 100 min (c,g) and 120 min (d,h). The CF spin rinsing speed is 6000 rpm.

The effects of CF rinsing as well as the ensuing annealing condition on the surface morphology and grain growth of the perovskite layers were characterized by scanning electron microscopy (SEM). Fig. 3(a-d) and Fig. 3(e-h) show the SEM top view and cross-sectional images of the differently treated perovskite films, respectively. From the top view images (Fig. 3(a-d)), it is obvious that both the surface coverage and roughness were greatly improved with CF rinsing. While the untreated perovskite film looks obviously platelet-like or texture-like (Fig. 3(a)), smooth and complete surface coverage for the CF treated perovskite layers at all annealing conditions was observed (Fig. 3(b-d)). Furthermore, from the cross-sectional SEM micrographs, the thickness of the CF rinsed perovskite layer was found to decrease initially, from 238 nm for the layer annealed for 80 min, with annealing time and then saturates at 212 ~ 213 nm after 100 min of thermal annealing (Fig. 3(e-h)). It is also remarkable that grains with size around 1 micron were observed for all CF rinsed perovskite layers. The results of atomic force microscopy (AFM) measurements were shown in Fig. 4(a-d). The surface roughness R_{rms} over an 50 $\mu m \times 50$ μm area was 72 nm for the untreated film, and was 26 nm, 32 nm and 32 nm for the CF rinsed films with ensuing annealed at 90°C for 80, 100 and 120 min, respectively. Figure 5 shows a perovskite layer of 8 cm × 8 cm prepared by CF rinsing. Mirror-like surface and high uniformity on the large scale are obviously observed.
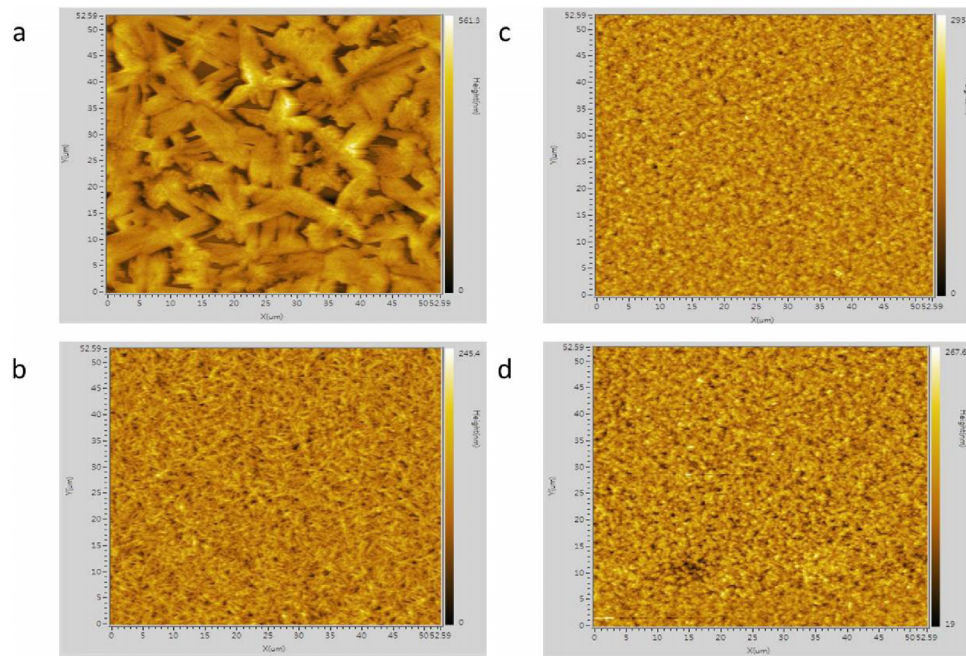
FIG. 4. AFM measurements from perovskite layers (a) annealed at 90°C for 100 min without CF treatment, and with CF soaking and rinsing followed by annealing at 90°C for 80 min (b), 100 min (c) and 120 min (d). The CF spin rinsing speed is 6000 rpm.

Planar PSCs with p-i-n layer structure comprising ITO/PEDOT:PSS (40nm) /perrovskite/ $PC_{61}BM$ (80 nm)/Al (100 nm) were fabricated to investigate the effects of CF rinsing on the photovoltaic performance. An array of 2 x 2 devices, each with an active area of 0.04 cm^2, was defined by the overlap of the ITO anodes and Al cathodes around the corner of the square-shaped perovskite films. These devices are at least 1 cm apart from one another and their *J-V* curves can thus be used to check the uniformity of the perovskite layers. A picture of a typical square-shaped CF treated
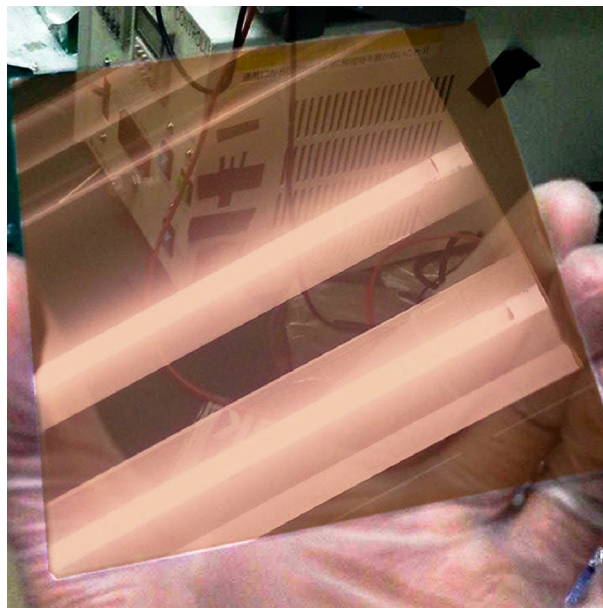

FIG. 5. A picture of a 8 cm × 8 cm perovskite layer prepared by CF rinsing, exhibiting mirror-like surface and high uniformity on the large scale.
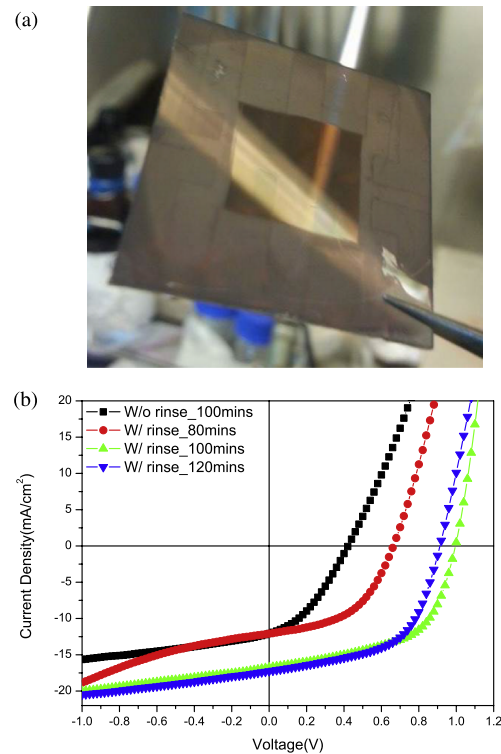
(a)

(b)

FIG. 6. (a) A picture of the annealed perovskite layers with PEDOT:PSS in peripheral regions removed by ACE to expose the ITO contact pads, revealing high uniformity on centimeter scale; (b) the *J-V* characteristics of PSCs fabricated with perovskite layers annealed at 90°C for 100 min without CF treatment (■), with CF soaking and rinsing at 6000 rpm followed by annealing at 90°C for 80 min (●), 100 min (▲) and (d) 120 min (▼), respectively.

perovskite layer and the measured *J-V* curves obtained from the fabricated PSCs with rinsing spinning at 6000 rpm and annealed at 90°C for different time duration are shown in Fig. 6. For comparison the *J-V* curve of an untreated reference device was also included. The corresponding photovoltaic parameters are summarized in Table I and their corresponding absorption and IPCEs can be found in Fig. 7. It is notable that, due to the high viscosity of DMSO and its retarding effects on reaction,[4] higher rotational speed in the spin coating of the precursor layer was found necessary to achieve higher efficiency for PSCs without CF rinsing. However, to study the effects of CF rinsing, the same rotational speed is used for the precursor spin coating of all these perovskite layers. The untreated PSC device was thus not optimized and a low PCE of 1.86% was observed. Although not included here, it is to note that a PCE of 8.5% was achieved for the untreated PSC prepared at a rotational speed of 8000 rpm for the precursor layer. From Fig. 6(b), it was found that the short-circuit current (J_{sc}) increases with the annealing time. On the other hand, the open-circuit voltage (V_{oc})

TABLE I. Summary of the photovoltaic parameters of PSC prepared with different rinsing speed and annealing time. Each data is obtained from 4 devices from the perovskite layer.

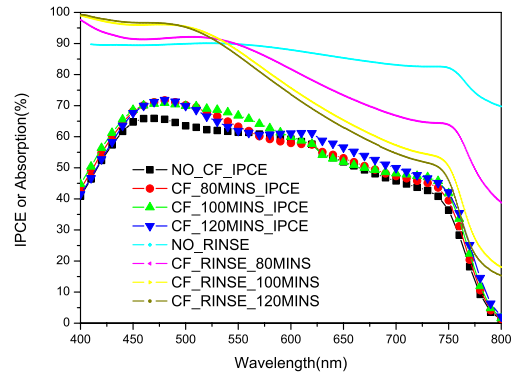| Spinning Speed (rpm)	Annealing time (min)	V_{oc} [V]	J_{sc} [mA/cm^2]	*FF* [%]	*PCE* [%]
NA	100	0.421	12.1	36.6	1.86
6000	80	0.67 ± 0.01	12.08 ± 0.83	49.05 ± 1.85	3.94 ± 0.34
6000	100	1.00 ± 0.01	16.75 ± 0.36	56.05 ± 1.06	9.35 ± 0.29
6000	120	0.92 ± 0.01	17.27 ± 0.3	56.00 ± 1.27	8.84 ± 0.26
1500	100	0.91 ± 0.01	16.26 ± 0.8	54.40 ± 3.12	8.05 ± 0.9
3000	100	1.04 ± 0.01	17.49 ± 0.25	58.90 ± 0.83	10.67 ± 0.13
4500	100	1.01 ± 0.02	15.91 ± 0.4	55.10 ± 0.67	8.88 ± 0.15

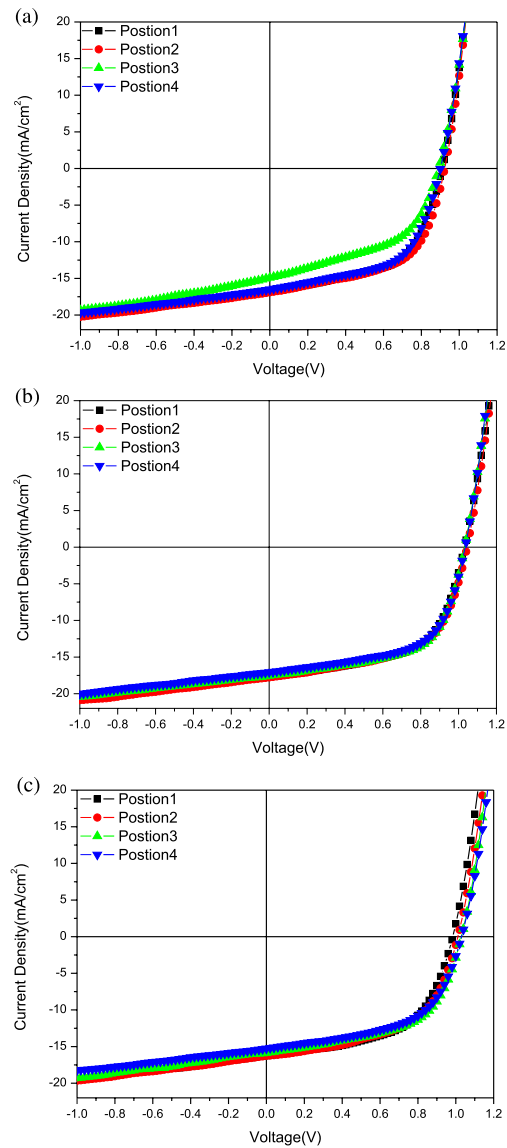FIG. 7. The corresponding absorption and IPCEs for the *J-V* curves shown in Fig. 6.

FIG. 8. The *J-V* characteristics of PSCs fabricated with CF treated perovskite layers with rinsing spinning at (a) 1500 rpm, (b) 3000 rpm and (c) 4500 rpm, followed by annealing at 90°C for 100 min.

TABLE II. The thickness of perovskite layer after annealing at 90°C for 100 min, prepared with different rotational speeds for the spin-coating of precursor solution and CF soaking and rinsing.

Precursor spin rate (rpm)	Spinning Speed (rpm)	Perovskite thickness (nm)
4000	3000	218
5000	3000	218
6000	3000	215
7000	3000	222
6000	NA	283
6000	1500	218
6000	3000	220
6000	4500	199
6000	6000	175

increases initially with the annealing time, reaches a maximum value of 1.01 V for the case with 100 min annealing and then decreases with further annealing, similar to what was reported in the literature.[23] The increase in J_{sc} as well as V_{oc} with annealing time may be attributed to the enlarged grain size and phase evolution.[23] The reduced V_{oc} due to excessive annealing may be ascribed to either the increase in surface roughness which leads to increased leakage (Fig. 4) or the reduction of residual high-bandgap $CH_3NH_3PbCl_3$ surface precipitation layer (Fig. 3(c) and Fig. 3(d)).

After optimizing the annealing time, we proceed to investigate the effects of rinsing spinning speed. Fig. 8(a), 8(b) and 8(c) display the measured J-V curves taken from PSCs with CF spinning at 1500, 3000 and 4500 rpm, respectively. The four J-V curves in each plot were taken from those 4 devices fabricated on the same perovskite film. It is remarkable that almost coincident J-V curves were obtained when the CF spinning speed is 3000 and 4500 rpm. Very high uniformity in the perovskite layers on centimeter scale was observed at high rinsing spinning speeds.

This observed high uniformity is closely related to one of the salient points of this soaking and surface rinsing scheme, as compared to the original solvent washing method, that the thickness of resulted films is predominantly determined by the rinsing spinning speed when it is more than 1500 rpm. As shown in Table II, precursor films spin-coated at rotational speed ranging from 4000 to 7000 rpm all yield to perovskite films of 220 nm after CF rinsing and an ensuing spinning at 3000 rpm followed by annealing at 90°C for 100 min. On the other hand, perovskite precursor films spin-coated at 6000 rpm were found to produce perovskite layers of different thickness depending on the CF rinsing spinning speed. It is also notable that at the CF rinsing spinning speed of 3000 rpm, a maximum PCE of 10.6 ± 0.2% was achieved. Furthermore, the evolution of the photovoltaic performance of CF rinsed PSCs with time was monitored continuously and the results were shown in Fig. 9. It was found that these CF treated PSCs exhibit much prolonged lifetime
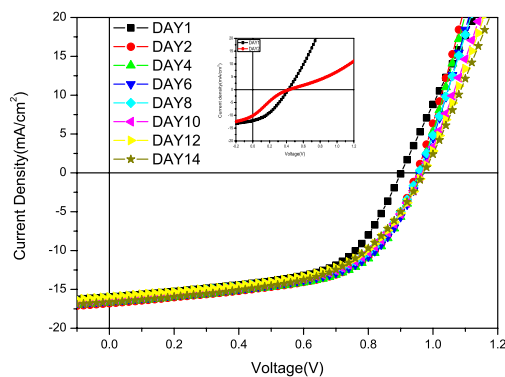

FIG. 9. Evolution of J-V curves of PSCs fabricated with CF treated perovskite layers with rinsing spinning 3000 rpm, followed by annealing at 90°C for 100 min. For comparison, the results from untreated reference PSC was included as inset.

TABLE III. Summary of the photovoltaic parameters of PSC measured after its fabrication, corresponding to the *J*-*V* curves shown in Fig. 6.

		V_{oc} [V]	J_{sc} [mA/cm^2]	*FF* [%]	*PCE* [%]
w/o rins	Day1	0.42	12.07	0.37	1.87
	Day2	0.43	10.136	21.1	0.92
w/rins.	Day1	0.9	15.97	57.9	8.33
	Day2	0.95	16.78	57.7	9.194
	Day4	0.96	16.69	57.8	9.24
	Day6	0.96	16.44	57.1	9.03
	Day8	0.96	16.145	56.6	8.75
	Day10	0.97	16.48	55.3	8.8
	Day12	0.97	15.98	55.2	8.54
	Day14	0.97	16.64	54	8.721

with the PCE retaining more than 90% of its initial value even after 14 days (See also Table III). As a comparison, the photovoltaic performance of the untreated PSCs degraded greatly, even on the second day, as shown in the inset in Fig. 9.

It is interesting to compare the use of toluene and CF as rinsing solvent. PSCs of the same structure were fabricated with identical process, albeit with toluene as rinsing solvent. A picture of the toluene treated perovskite layer just after the thermal annealing and the *J*-*V* curve of the toluene rinsed device with the highest PCE of 12% were shown in Fig. 10. Although the best toluene rinsed device exhibits higher PCE than that with CF treatment, compromised large-area uniformity in the perovskite layer was found.

The much improved large-area uniformity achieved with CF as rinsing solvent, as compared to toluene, can be understood by noting that CF, because of its smaller molar volume and lower
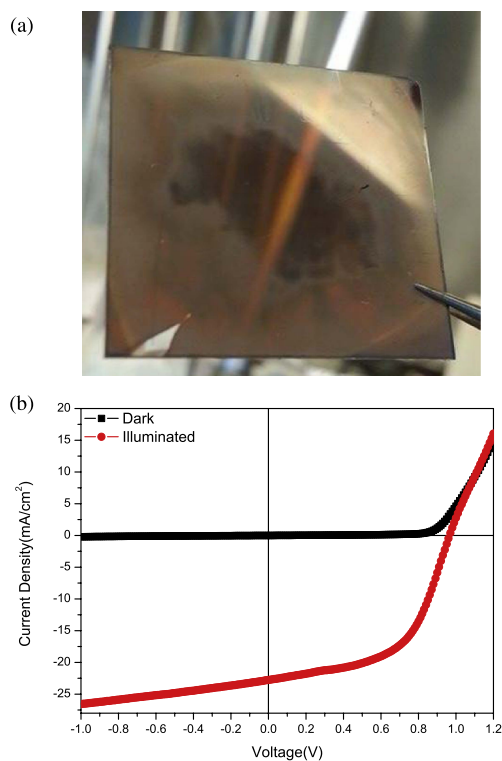

FIG. 10. (a) A picture of the annealed perovskite layers with toluene treatment, showing compromised uniformity on centimeter scale; (b) the *J*-*V* characteristics of a toluene treated PSC with the best photovoltaic performance.

viscosity, can mix with DMSO:DMF mixture more quickly than toluene.[24] Therefore, CF can decrease the viscosity of the precursor solution more feasibly, leading to more uniform perovskite layers with the ensuing spinning. Reduced viscosity due to the CF mixing explains also the predominant dependence of perovskite film thickness on the CF rinsing spinning speed (Table II). Finally, the much prolonged lifetime may also be due to the feasibility of mixing between CF and DMSO:DMF. According to Xie *et al*, the removal of CH_3NH_3Cl (MACl) improves greatly the device stability.[18] Since the mixing of CF helps to remove the DMF:DMSO mixture used for the precursor solution by reducing the solution viscosity, as exhibited by the predominant dependence of perovskite layer thickness on the rinsing spinning speed, it may also help to remove unreacted MACl dissolved in DMSO/DMF mixture. More studies are needed to investigate this possibility of chemical removal of MACl for improved reliability.

IV. CONCLUSIONS

In conclusion, a solvent soaking and rinsing method, in which the solvent was allowed to soak all over the surface, was found to lead to perovskite layers with high uniformity on a large scale and much enhanced reliability. With CF as rinsing solvent, highly uniform PSCs with prolonged lifetime were demonstrated. The uniformity and reliability with this solvent soaking and rinsing method were ascribed to the low viscosity of CF and its feasible mixing with DMSO:DMF. Because of the uniformity and reliability, CF soaking and rinsing may be useful for the fabrication of large-area planar PSCs.

ACKNOWLEDGEMENTS

[1] H. J. Snaith, J. Phys. Chem. Lett. **4**, 3623 (2013).
[2] http://www.nrel.gov/ncpv/, NREL, Best Research-Cell Efficiencies, http://www.nrel.gov/ncpv/images/efficiency_chart.jpg, accessed: 2, 2015.
[3] J. Burschka, N. Pellet, S. J. Moon, R. Humphry-Baker, P. Gao, M. K. Nazeeruddin, and M. Grätzel, Nature. **499**, 316 (2013).
[4] N. J. Jeon, J. H. Noh, Y. C. Kim, W. S. Yang, S. Ryu, and S. l. Seok, Nature Materials. **13**, 897 (2014).
[5] J. You, Z. Hong, Y. (Michael) Yang, Q. Chen, M. Cai, T. B. Song, C. C. Chen, S. Lu, Y. Liu, H. Zhou, and Y. Yang, ACS Nano. **8**, 1674 (2014).
[6] J. W. Jung, S. T. Williamsa, and A. K. Jen, RSC Adv. **4**, 62971 (2014).
[7] M. Liu, M. B. Johnston, and H. J. Snaith, Nature. **501**, 395 (2013).
[8] C. W. Chen, H. W. Kang, S. Y. Hsiao, P. F. Yang, K. M. Chiang, and H. W. Lin, Adv. Mater. **26**, 6647 (2014).
[9] Q. Chen, H. Zhou, Z. Hong, S. Luo, H. S. Duan, H. H. Wang, Y. Liu, G. Li, and Y. Yang, J. Am. Chem. Soc. **136**, 622 (2014).
[10] G. E. Eperon, V. M. Burlakov, P. Docampo, A. Goriely, and H. J. Snaith, Adv. Funct. Mater. **24**, 151 (2014).
[11] J. Seo, S. Park, Y. C. Kim, N. J. Jeon, J. H. Noh, S. C. Yoon, and S. l. Seok, Energy Environ. Sci. **7**, 2642 (2014).
[12] H. Zhou, Q. Chen, G. Li, S. Luo, T. B. Song, H. S. Duan, Z. Hong, J. You, Y. Liu, and Y. Yang, Science. **345**, 542 (2014).
[13] R. Kang, J. E. Kim, J. S. Yeo, S. Lee, Y. J. Jeon, and D. Y. Kim, J. Phys. Chem. C. **118**, 26513 (2014).
[14] J. You, Y. Yang, Z. Hong, T. B. Song, L. Meng, Y. Liu, C. Jiang, H. Zhou, W. H. Chang, G. Li, and Y. Yang, Appl. Phys. Lett. **105**, 183902 (2014).
[15] B. Conings, L. Baeten, C. D. Dobbelaere, J. D'Haen, J. Manca, and H. G. Boyen, Advanced Materials. **26**, 2041 (2014).
[16] Z. Xiao, Q. Dong, C. Bi, Y. Shao, Y. Yuan, and J. Huang, Adv. Mater. **26**, 6503 (2014).
[17] C. H. Chiang, Z. L. Tseng, and C. G. Wu, J. Mater. Chem. A **2**, 15897 (2014).
[18] F. X. Xie, D. Zhang, H. Su, X. Ren, K. S. Wong, M. Grätzel, and W. C. H. Choy, ACS Nano. **9**, 639 (2015).
[19] B. W. Park, B. Philippe, T. Gustafsson, K. Sveinbjörnsson, A. Hagfeldt, E. M. J. Johansson, and G. Boschloo, Chem. Mater. **26**, 4466 (2014).
[20] C. C. Chen, S. H. Bae, W. H. Chang, Z. Hong, G. Li, Q. Chen, H. Zhou, and Y. Yang, Mater. Horiz. **2**, 203 (2015).
[21] L. Daniels, Chem. Eng. **102**, 70-78 (1995).
[22] P. A. M. Boomkamw and R. H. M. Miesew, Int. J. Multiphase Flow. **22**, 67 (1996).
[23] T. B. Song, Q. Chen, H. Zhou, S. Luo, Y. Yang, J. You, and Y. Yang, Nano Energy. **12**, 494 (2015).
[24] Wilke and Wang, AIChE Journal. **1**, 264 (1955).